Formal Analysis of Abnormal Excitation in Cardiac Tissue

Pei Ye[1], Scott A. Smolka[1], Radu Grosu[1], and Emilia Entcheva[2]

[1] Computer Science Department, Stony Brook University, NY 11794, USA
[2] Biomedical Engineering Department, Stony Brook University, NY 11794, USA

Abstract. We present the Piecewise Linear Approximation Model of Ion Channel contribution (PLAMIC) to cardiac excitation. We use the PLAMIC model to conduct formal analysis of cardiac arrhythmic events, namely Early Afterdepolarizations (EADs). The goal is to quantify (for the first time) the contribution of the overall sodium (Na^+), potassium (K^+) and calcium (Ca^{2+}) currents to the occurrence of EADs during the plateau phase of the cardiac action potential (AP). Our analysis yields exact mathematical criteria for the separation of the parameter space for normal and EAD-producing APs, which was validated by simulations with classical AP models based on complex systems of nonlinear differential equations. Our approach offers a simple formal technique for the prediction of conditions leading to arrhythmias (EADs) from a limited set of experimental measurements, and can be invaluable for devising new anti-arrhythmic strategies.

1 Introduction

Excitable cells are those cells capable of generating and propagating electrical signals without damping. They are essential biological building blocks, determining functionality in the brain, heart, skeletal and smooth muscles.

An *action potential* (AP) is a change in an excitable cell's membrane potential caused by the flow of different ions across the cell membrane. The left panel in Fig. 1 illustrates a normal AP waveform for a guinea-pig heart cell. By convention, a normal AP follows a well defined cycle of "depolarization" (the rising phase), followed by "repolarization" (the falling phase). Furthermore, in qualitative terms, the "repolarization" phase can be divided in "early repolarization", "plateau" and "final repolarization".

Under some pathological conditions leading to a prolonged repolarization phase, the morphology of the AP can be altered by an abnormal secondary depolarization, termed **Early Afterdepolarization** (EAD). By clinical definition [3, 4], EADs occur before the completion of repolarization of an AP (as illustrated in the right panel of Fig. 1).

Such cellular-level events can give rise to undesired new excitation waves and can precipitate life-threatening heart activation sequences, e.g. tachyarrhythmias, especially in patients with Long QT syndrome [5, 8]. As critical arrhythmia triggers, EADs have been of interest to cardiac researchers for several

decades [11]. Attempts have been made to uncover the ionic mechanisms underlying EADs, so that their occurrence can be predicted as well as effectively treated. Various studies have found that the reactivation of calcium (Ca^{2+}) or sodium (Na^{+}) channels or abnormally reduced potassium (K^{+}) current can lead to this phenomenon [7, 2, 1]. Yet, a unified view of EAD mechanisms along with predictive criteria are lacking.

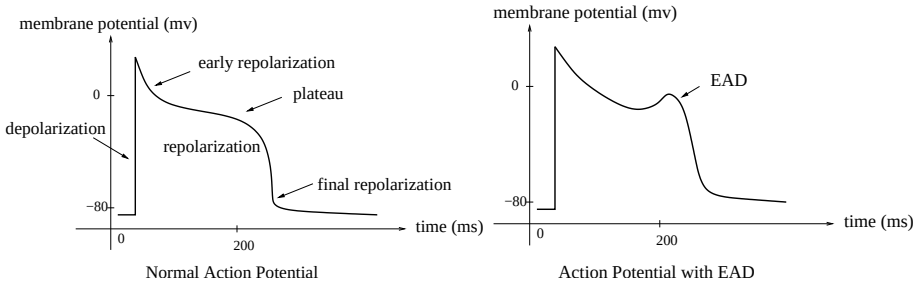

Fig. 1. EAD in cardiac myocyte.

In this paper, we present the *Piecewise Linear Approximation Model of the Ion Channel contribution* (PLAMIC) as a basis for understanding and analyzing the biochemical mechanisms underlying the formation of EADs during the cardiac action potential. The derivation of the PLAMIC model can be understood as follows. Let V^{Na^+}, $V^{Ca^{2+}}$ and V^{K^+} denote the integral contributions to the AP due to the sodium, calcium and potassium channels, respectively; i.e. the voltages the ionic currents flowing through these channels induce. Further, let V^{NaK} denote the combined sodium and potassium voltage.

A key observation is that during normal and abnormal APs, the behavior of $V^{Ca^{2+}}$ and V^{NaK} corresponds to triangular-like functions of opposite polarity (see Fig. 3). As such, in the PLAMIC model, $V^{Ca^{2+}}$ and V^{NaK} are approximated in a piecewise-linear fashion using two very simple triangular functions, each of which naturally comprises a rising phase and a falling phase. The PLAMIC model also incorporates an AP-morphology-related (exponential) decay function, which can be fitted across different cell types.

A main advantage of the PLAMIC model then is its highly constrained parameter space, essentially limited to the peak voltage values and their occurrence in time of the two triangular functions. The model is therefore amenable to a closed-form, voltage-monotonicity analysis on the AP cycle during repolarization. We in fact show that the absence of a monotonically decreasing AP V ($\frac{dV}{dt} < 0$) during the plateau phase of repolarization is a necessary and sufficient condition for EAD. We furthermore provide specific conditions on the parameter space (involving the relative slopes of the two triangular functions, the relative occurrence of their peaks, and their relative magnitudes) for EAD occurrence.

We also performed an experimental validation of the conditions derived from the above-described formal analysis of the PLAMIC parameter space, assembling

a test set of normal and abnormal APs from the widely accepted Luo-Rudy model ventricular cell model [9]. Our results demonstrate that the results of our formal analysis can be used as a valid classifier for EAD prediction.

The organization of the rest of the paper is as follows: Section 2 provides a formal definition of the PLAMIC model. Section 3 conducts a model-based analysis of the conditions under which EADs occur. Section 4 uses computer simulations with the Luo-Rudy model to validate our results. Section 5 offers our concluding remarks and directions for future work.

2 The PLAMIC Model

Mathematical modeling of excitable cells has a long tradition, starting with the first empirically-derived ionic model of the action potential in a giant squid axon proposed by Hodgkin and Huxley in 1952 [6]. Subsequently, more ion channels and complex biophysical processes have been included in these models, although the general mathematical framework for representing the ion-channel contribution has remained essentially the same.

The model we propose adopts an abstraction based on voltage, i.e., it deals with the superposition of the voltages generated by the individual ion channels. We study the occurrence of EADs as a disturbance in the subtle balance between the underlying ion currents using their voltage surrogates.

The advantage of using superposition of the voltages, as opposed to the ionic currents directly, is the integral (smoother) nature of the former in the RC-circuit model that approximates the electrical behavior of the cell membrane. This facilitates the curve-fitting process and allows for simpler mathematical expressions to be employed and further linearized in a piecewise fashion. The result is the *Piecewise Linear Approximation Model of the Ion-Channel contributions* (PLAMIC).

We illustrate the idea of the PLAMIC model starting from a modification of traditional ionic models based on the Hodgkin-Huxley formalism. The main equation used in these ionic models is presented in Eqn. 1.

$$C\dot{V} = -\sum I_{\mathrm{i}}(t) + I_{\mathrm{st}}(t) \tag{1}$$

where $\dot{v}$ is the time derivative of the membrane potential V, C is the equivalent capacitance of the cell membrane; $\sum I_i(t)$ is the sum of all the ion currents flowing in or out of the cell membrane; $I_{\mathrm{st}}(t)$ is the stimulation current.

$\sum I_i(t)$ may incorporate a number of individual currents for different cell types. For example, in the Luo-Rudy model [9] (LRd), a widely accepted ventricular cell model, currents can be grouped by ion species as in Eqn. 2.

$$\sum I_{\mathrm{i}}(t) = I_{\mathrm{Na}}(t) + I_{\mathrm{K}}(t) + I_{\mathrm{Ca}}(t) \tag{2}$$

where I_{Na}, I_{K}, and I_{Ca} are the sodium, potassium and calcium overall ion currents, respectively. The top row of Fig. 2 plots these three components of the LRd model for a normal AP.

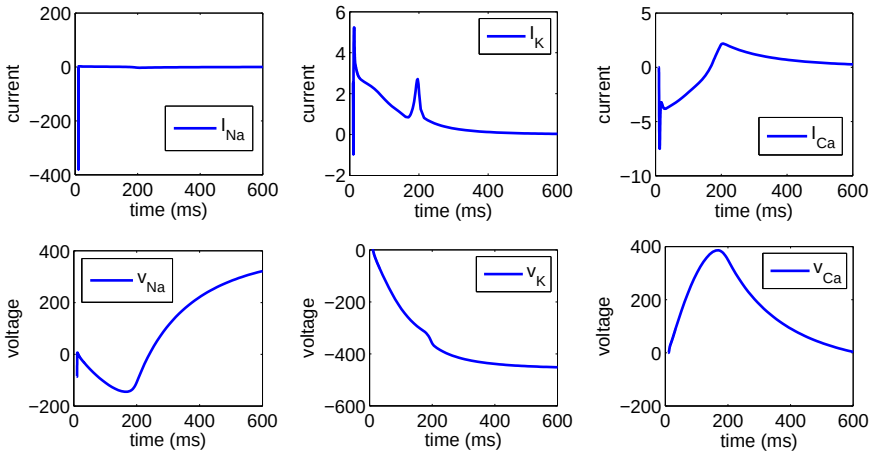

Fig. 2. Individual ionic currents and their corresponding voltages in the LRd model.

Using for each component current the corresponding voltage, Eqns. 1 and 2 can be equivalently rewritten into the following form (Eqn. 3):

$$\begin{gathered} C\dot{V}_{\mathrm{Na}} = -I_{\mathrm{Na}}(t), C\dot{V}_{\mathrm{K}} = -I_{\mathrm{K}}(t) \\ C\dot{V}_{\mathrm{Ca}} = -I_{\mathrm{Ca}}(t), C\dot{V}_{\mathrm{st}} = I_{\mathrm{st}}(t) \\ V = (V_{\mathrm{Na}}(t) + V_{\mathrm{K}}(t) + V_{\mathrm{Ca}}(t)) + V_{\mathrm{st}}(t) \end{gathered} \tag{3}$$

where V_{Na}, V_{K}, V_{Ca} and V_{st} are the voltages obtained via integration from I_{Na}, I_{K}, I_{Ca} and I_{st}, respectively.

The motivation behind Eqn. 3 is to first calculate the voltages from the individual currents and then obtain the overall membrane potential via superposition. Note the much smoother appearance of the voltage curves (bottom row) compared to the "spikey" current curves (top row) in Fig. 2. Furthermore, grouping the sodium and potassium voltages into one combined voltage yields the opposing triangular-like (and thus inherently linearizable) voltage functions depicted in Fig. 3.

The essentially triangular-shaped voltage functions suggests the use of two linear segments (linked together in a triangular form) to approximate the combination voltage due to the sodium and potassium currents (denoted as the NaK voltage), and the individual voltage due to the calcium current alone (the Ca voltage).

2.1 Definition of the PLAMIC Model

Two linear segments, forming a triangle (also known as a lagrange hat function), are used to represent each of the NaK and Ca voltages. Two of the triangle vertices (beginning and end) are fixed on the time-axis and the triangle shape varies by shift in the free (peak) vertex. The triangular function is shown in

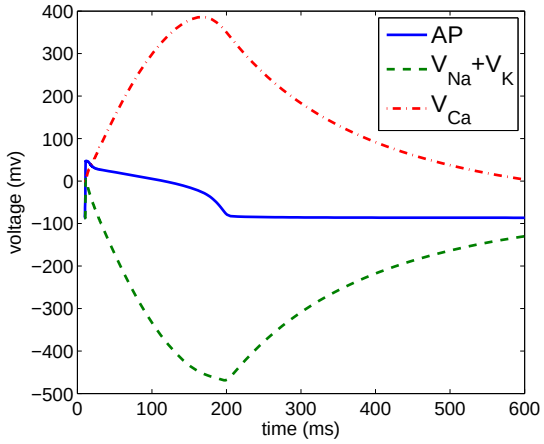

Fig. 3. AP, combined sodium and potassium voltage, and calcium voltage in LRd model.

Fig. 4 (A). It is essentially a two-piece linear function starting from point $(0, 0)$ and ending at $(T_S, 0)$, where T_S is the total simulation time for the generation of an AP.

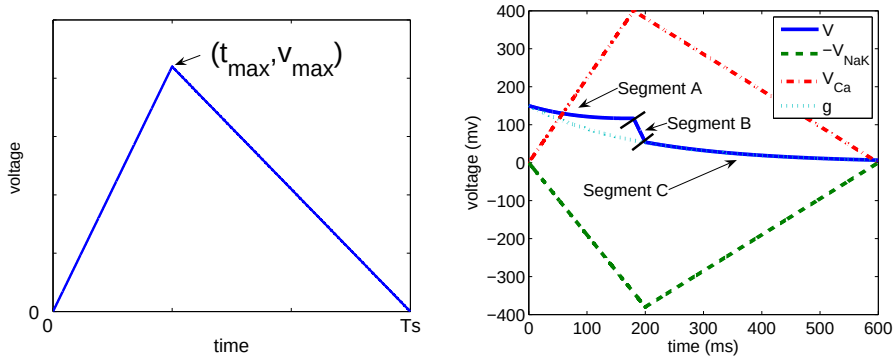

(A) The triangular function. (B) The PLAMIC model.

Fig. 4.

By fixing the simulation time T_S, each function is determined solely by the switching (peak) point $(t_{\max}, v_{\max})$. The mathematical definition of the triangular function is given by Eqn. 4, where the superscript $u \in \{Ca, NaK\}$ is used to distinguish the voltage functions corresponding to the different current types.

$$f^u(t) = \begin{cases} \frac{v^u_{\max}}{t^u_{\max}} t, & t \le t^u_{\max}; \\ \\ \frac{T_S - t}{T_S - t^u_{\max}} v^u_{\max}, & t^u_{\max} < t \le T_S. \end{cases} \tag{4}$$

The functions for v_{Ca} and v_{NaK} are then defined simply as follows:

$$v_{\mathrm{Ca}}(t) = f^{\mathrm{Ca}}(t) \tag{5}$$

$$v_{\mathrm{NaK}}(t) = f^{\mathrm{NaK}}(t) \tag{6}$$

The overall action potential v is the superposition of the two (Eqn. 7).

$$v(t) = v_{\mathrm{Ca}}(t) - v_{\mathrm{NaK}}(t) + g(t) \tag{7}$$

where $g(t)$ is a decay function related to the AP morphology. It is defined by $V_{\max}$, the absolute difference between the resting potential and the maximum voltage during upstroke, and by D ($D < 0$), an action-potential-duration parameter which can be adjusted across different cell types (Eqn. 8).

$$g(t) = V_{\max} e^{\mathrm{D}t} \tag{8}$$

The decay function qualitatively reflects the passive component of the cell-membrane response: an RC circuit will exhibit exponential decay after the upstroke due to capacitor discharge. In the PLAMIC model, this passive decay is used in conjunction with the superposed opposite potentials (NaK and Ca).

Based on the relative magnitude of $t^{\mathrm{Ca}}_{\max}$ and $t^{\mathrm{NaK}}_{\max}$ (i.e. which voltage reaches its peak first), the AP equation for v (Eqn. 7) has two alternative formulations. In each case, v is represented as a three-segment function, referred to in the following equations as segments A, B and C, respectively.

First, let $a^{\mathrm{c}}_1 = \frac{v^{\mathrm{Ca}}_{\max}}{t^{\mathrm{Ca}}_{\max}}$, $a^{\mathrm{c}}_2 = \frac{-v^{\mathrm{Ca}}_{\max}}{T_S - t^{\mathrm{Ca}}_{\max}}$, $b^{\mathrm{c}} = \frac{v^{\mathrm{Ca}}_{\max}}{T_S - t^{\mathrm{Ca}}_{\max}} T_S$, $a^{\mathrm{k}}_1 = \frac{v^{\mathrm{NaK}}_{\max}}{t^{\mathrm{NaK}}_{\max}}$, $a^{\mathrm{k}}_2 = \frac{-v^{\mathrm{NaK}}_{\max}}{T_S - t^{\mathrm{NaK}}_{\max}}$, and $b^{\mathrm{k}} = \frac{v^{\mathrm{NaK}}_{\max}}{T_S - t^{\mathrm{NaK}}_{\max}} T_S$.

Case I: $t^{\mathrm{Ca}}_{\max} < t^{\mathrm{NaK}}_{\max}$

$$v(t) = \begin{cases} a^{\mathrm{c}}_1 t - a^{\mathrm{k}}_1 t + V_{\max} e^{\mathrm{D}t}, & t \le t^{\mathrm{Ca}}_{\max}, \text{ segment A}; \\ (a^{\mathrm{c}}_2 t + b^{\mathrm{c}}) - a^{\mathrm{k}}_1 t + V_{\max} e^{\mathrm{D}t}, & t^{\mathrm{Ca}}_{\max} < t \le t^{\mathrm{NaK}}_{\max}, \text{ segment B}; \\ (a^{\mathrm{c}}_2 t + b^{\mathrm{c}}) - (a^{\mathrm{k}}_2 t + b^{\mathrm{k}}) + V_{\max} e^{\mathrm{D}t}, & t \ge t^{\mathrm{NaK}}_{\max}, \text{ segment C}. \end{cases} \tag{9}$$

Case II: $t^{\mathrm{Ca}}_{\max} \ge t^{\mathrm{NaK}}_{\max}$

$$v(t) = \begin{cases} a^{\mathrm{c}}_1 t - a^{\mathrm{k}}_1 t + V_{\max} e^{\mathrm{D}t}, & t \le t^{\mathrm{NaK}}_{\max}, \text{ segment A}; \\ a^{\mathrm{c}}_1 t - (a^{\mathrm{k}}_2 t + b^{\mathrm{k}}) + V_{\max} e^{\mathrm{D}t}, & t^{\mathrm{NaK}}_{\max} < t \le t^{\mathrm{Ca}}_{\max}, \text{ segment B}; \\ (a^{\mathrm{c}}_2 t + b^{\mathrm{c}}) - (a^{\mathrm{k}}_2 t + b^{\mathrm{k}}) + V_{\max} e^{\mathrm{D}t}, & t \ge t^{\mathrm{Ca}}_{\max}, \text{ segment C}. \end{cases} \tag{10}$$

In Fig. 4 (B), one of the possible implementations of the PLAMIC model (case I) is shown. The overall PLAMIC-abstracted AP is given as a solid line, with its three segments annotated accordingly. We plot $-v_{\mathrm{NaK}}$ instead of v_{NaK} to reveal the similarity to the LRd AP parameters shown in Fig. 3.

3 Formal Analysis of the PLAMIC Model

3.1 Monotonicity and EADs

EADs are secondary depolarization phenomena that arise during the repolarization phase; i.e. they disrupt the normal voltage return to rest. Therefore, a monotonicity analysis of the AP is an appropriate test for EADs. For example, it is safe to claim that a monotonically decreasing AP v ($\frac{dv}{dt} < 0$) is a sufficient condition for the absence of EADs. The opposite statement does not always hold, i.e. it is *not* always the case that if AP v is not universal decreasing, there is an EAD. For example, a "notch" in the early repolarization phase is common in many cardiac cells and is not considered an EAD (Fig. 5 (A)). Furthermore, in some cases, the membrane may transiently hyperpolarize; i.e. an undershoot may occur, with the potential lower than the resting potential during final repolarization. This non-monotonic case is also not an EAD (Figure 5 (B)).

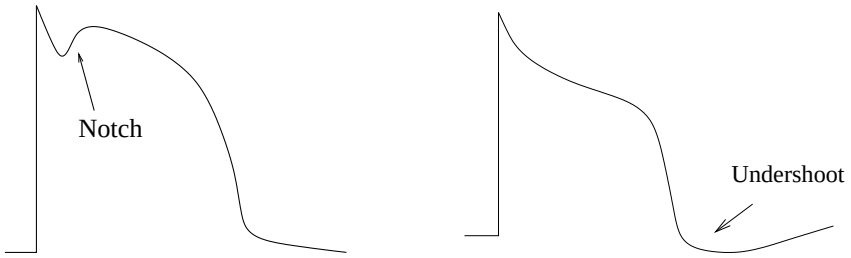

(A) Notch during early repolarization. (B) Undershoot during final repolarization.

Fig. 5. Non-monotonic APs that do not exhibit EADs.

If, however, the monotonicity analysis is restricted to the "plateau" phase of the repolarization process, any deviation from monotonic decay will effectively be an EAD. In order to define the plateau phase in the PLAMIC model, let *notch-delay* be the cell-type-specific initial time segment of the repolarization phase during which a notch may occur. The PLAMIC plateau phase is then defined to consist of the suffix of segment A beginning at *notch-delay* followed by segment B. For most physiological choices of $(t^u_{\max}, v^u_{\max})$, $u \in \{Ca, NaK\}$, this definition of the plateau phase coincides closely with its physiological counterpart.

Based on the above monotonicity discussion, the following definition will serve as the theoretical basis of our formal analysis of EAD in the PLAMIC model.

Definition 1. *The PLAMIC model contains an* EAD *if* $\frac{dv}{dt} > 0$ *at some point during the plateau phase.*

In Section 3.2, we present a monotonicity analysis of the PLAMIC plateau phase for both Cases I and II, and derive the exact conditions for EAD occurrence. Physiological explanations for these conditions are discussed as well.

3.2 Monotonicity Analysis of the PLAMIC Model

Case I Case I is the most physiologically feasible scenario in cardiac cells. In simulation data of normal cardiac APs using the LRd model, $t_{\max}^{\mathrm{Ca}} < t_{\max}^{\mathrm{NaK}}$ holds at all times. As the PLAMIC-based voltage is a piecewise-linear function, monotonicity is analyzed on a per-segment basis.

Segment A The first derivative of v within this segment is given by the following equation

$$\frac{dv}{dt} = a_1^{\mathrm{c}} - a_1^{\mathrm{k}} + V_{\max} D e^{\mathrm{Dt}} \tag{11}$$

Imposing the condition $\frac{dv}{dt} > 0$ yields:

$$t > \frac{1}{D} \ln(\frac{a_1^{\mathrm{k}} - a_1^{\mathrm{c}}}{V_{\max} D}) \tag{12}$$

Further examination of Eqn. 12 shows that the existence of a positive real solution for t requires the following conditions to hold:

$$\begin{cases} a_1^{\mathrm{c}} > a_1^{\mathrm{k}} > 0 \\ 0 < \frac{a_1^{\mathrm{k}} - a_1^{\mathrm{c}}}{V_{\max} D} < 1 \\ t < t_{\max}^{\mathrm{Ca}} \end{cases}$$

which are summarized in Theorem 1 as the major result for case I.

Theorem 1. $(a_1^{\mathrm{k}} < a_1^{\mathrm{c}} < (a_1^{\mathrm{k}} - V_{\max} D)) \wedge (t_{\max}^{\mathrm{Ca}} > \frac{1}{D} \ln(\frac{a_1^{\mathrm{k}} - a_1^{\mathrm{c}}}{V_{\max} D}))$ *is a sufficient condition for a case-I occurrence of EAD during the suffix of segment A beginning at notch-delay.*

In Fig. 6, we plot the different possibilities of the relative magnitudes of a_1^{k} and a_1^{c}. Table 1 summarizes the relationship between these values and the occurrence of EAD.

Condition	EAD	No EAD
$a_1^{\mathrm{c}} < a_1^{\mathrm{k}}$		Fig. 6 (A)
$a_1^{\mathrm{k}} < a_1^{\mathrm{c}} < a_1^{\mathrm{k}} - V_{\max} D$	Fig. 6 (D)	Fig. 6 (C)
$a_1^{\mathrm{k}} - V_{\max} D < a_1^{\mathrm{c}}$	Fig. 6 (B)	

Table 1. Summary of conditions for the existence of EAD in segment A.

An intuitive physiological explanation of the above result is that the existence of EAD is closely related to the relative speeds of the voltage increase due to different ion currents, represented by a_1^{c} and a_1^{k}.

At the beginning of the plateau phase, the AP follows a decreasing trend, which requires the calcium current to have an upper bound ($a_1^{\mathrm{c}} < a_1^{\mathrm{k}} - V_{\max} D$);

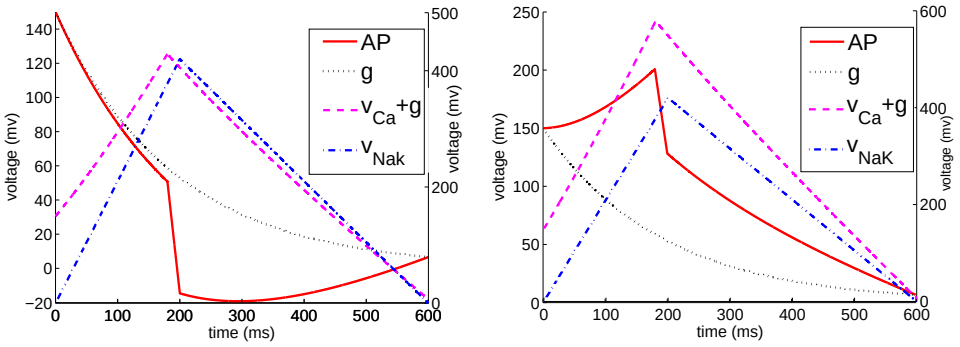

(A) $a_1^{\mathrm{c}} < a_1^{\mathrm{k}}$, no EAD

(B) $a_1^{\mathrm{k}} - V_{\max} D < a_1^{\mathrm{c}}$, EAD

(C) $a_1^{\mathrm{k}} < a_1^{\mathrm{c}} < a_1^{\mathrm{k}} - V_{\max} D$ and $t_{\max}^{\mathrm{Ca}} \leq \frac{1}{D} \ln(\frac{a_1^{\mathrm{k}} - a_1^{\mathrm{c}}}{V_{\max} D})$
No EAD

(D) $a_1^{\mathrm{k}} < a_1^{\mathrm{c}} < a_1^{\mathrm{k}} - V_{\max} D$ and $t_{\max}^{\mathrm{Ca}} > \frac{1}{D} \ln(\frac{a_1^{\mathrm{k}} - a_1^{\mathrm{c}}}{V_{\max} D})$
EAD

Fig. 6. PLAMIC-based analysis for EAD occurrence in segment A. The AP and decay functions are plotted as solid lines and use the y-axis on the left; v_{NaK} and $v_{\mathrm{Ca}} + decay$ are plotted in dashed lines and use the y-axis on the right. The same conventions apply to Figs. 7 and 8.

otherwise, the AP curve will be increasing through this segment. Furthermore, for an EAD to form, the balance has to be in favor of the calcium-current contribution ($a_1^{\mathrm{k}} < a_1^{\mathrm{c}}$). The last condition ensures that the calcium current has enough time to accumulate for the formation of an EAD ($t_{\max}^{\mathrm{Ca}} > \frac{1}{D}\ln(\frac{a_1^{\mathrm{k}}-a_1^{\mathrm{c}}}{V_{\max}D})$).

Segment B As in the analysis for segment A, we first determine the expression for $\frac{dv}{dt}$:

$$\frac{dv}{dt} = a_2^{\mathrm{c}} - a_1^{\mathrm{k}} + V_{\max}De^{\mathrm{Dt}} \tag{13}$$

Since $\frac{dv}{dt} < 0$ throughout this segment ($a_2^{\mathrm{c}} < 0$, $-a_1^{\mathrm{k}} < 0$ and $V_{\max}De^{\mathrm{Dt}} < 0$), no EAD is possible in segment B.

Case II The defining segment-A equation for v is exactly the same as in case I, modulo the replacement of $t_{\max}^{\mathrm{Ca}}$ with $t_{\max}^{\mathrm{NaK}}$ in the time bound for t. Following the case-I analysis for segment A, this observation yields the following condition for the occurrence of EADs:

$$\begin{cases} a_1^{\mathrm{c}} > a_1^{\mathrm{k}} > 0 \\ 0 < \frac{a_1^{\mathrm{k}}-a_1^{\mathrm{c}}}{V_{\max}D} < 1 \\ t < t_{\max}^{\mathrm{NaK}} \end{cases}$$

Similarly, the major result for Case II can be summarized as follows.

Theorem 2. *$(a_1^{\mathrm{k}} < a_1^{\mathrm{c}} < (a_1^{\mathrm{k}} - V_{\max}D)) \wedge (t_{\max}^{\mathrm{NaK}} > \frac{1}{D}\ln(\frac{a_1^{\mathrm{k}}-a_1^{\mathrm{c}}}{V_{\max}D}))$ is a sufficient condition for a case-II occurrence of EAD during the suffix of segment A beginning at notch-delay.*

For segment B, the first derivative of v is given by the following equation.

$$\frac{dv}{dt} = a_1^{\mathrm{c}} - a_2^{\mathrm{k}} + V_{\max}De^{\mathrm{Dt}} \tag{14}$$

As $a_1^{\mathrm{c}} > 0$ and $a_2^{\mathrm{k}} < 0$, and $a_1^{\mathrm{c}} - a_2^{\mathrm{k}} + V_{\max}De^{\mathrm{Dt}} > 0$ for typical values of $V_{\max}$ and C, we observe an increasing AP during this segment. Thus, by Definition 1, segment B always has case-II EAD. Based on whether or not segment A has EAD, two cases are possible: EAD commences in (the tail end of) segment A or it commences in segment B; see Fig. 7.

Although this particular EAD morphology was not observed in the computer simulations we performed with the LRd model, this does not preclude its actual occurrence. Further examination of experimental data is needed to confirm or deny the physiological relevance of this case.

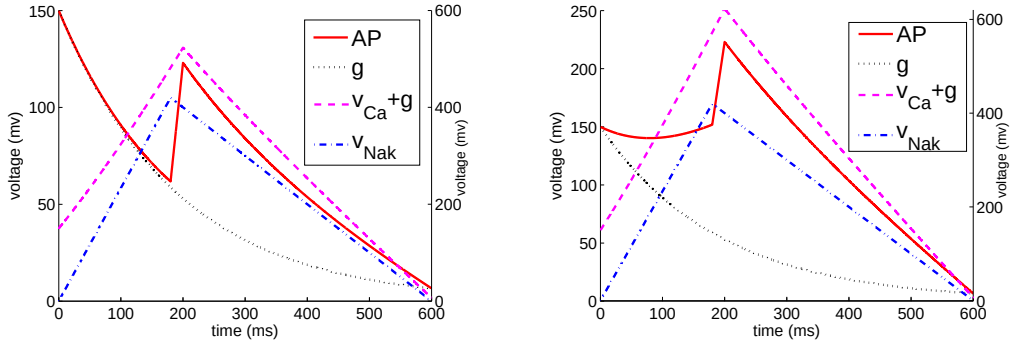

(A) Segment A has no EAD and Segment B has EAD. (B) Segments A and B both have EAD.

Fig. 7. The existence of Case-II EAD for segment B.

4 Experimental Validation of the PLAMIC Model

In this section, we consider the experimental validation of the PLAMIC model, specifically, the validity of Theorem 1 as an EAD predictor (classification rule) during the plateau phase of the AP cycle. To this end, we applied the protocols presented in [11] to the LRd cardiac-myocyte model to reproduce a number of AP curves with EADs. We also obtained the corresponding voltages for the calcium and the combined sodium and potassium currents using the integration method of Eqn. 3.

For each AP, in order to obtain the PLAMIC model parameters $(t^u_{\max}, v^u_{\max})$, $u \in \{Ca, NaK\}$, we took the maximum value of $V_{\mathrm{Na}} + V_{\mathrm{K}}$ as $v^{\mathrm{NaK}}_{\max}$, and the time at which it occurs as $t^{\mathrm{NaK}}_{\max}$. Data points $(t^{\mathrm{Ca}}_{\max}, v^{\mathrm{Ca}}_{\max})$ were obtained in a similar fashion. The constant coefficients in our experiments are defined as $V_{\max} = 150$, *offset*=127 (defined below), and $D = -0.0052$. These values have been chosen to match the LRd simulation results, but can be varied to fit different AP morphologies and cell types.

A side-by-side comparison of the AP curves obtained from the LRd and PLAMIC models for both normal and EAD-producing APs is illustrated in Fig. 8. The top-left panel shows a normal AP and an EAD-exhibiting AP, triggered by a calcium-current-enhancing drug, Bay K 8644. The top-right panel shows the PLAMIC model simulation for the two cases, which uses a piecewise-linear approximation of the current-inducing voltages obtained from the LRd model. The bottom row shows similar results for the LRd and PLAMIC models for EADs induced by the administration of cesium, resulting in a substantial prolongation of the repolarization phase.

The AP curves generated by the PLAMIC model qualitatively match the LRd curves, with an AP morphology that is more stylized due to the simplicity of the linear functions on which the PLAMIC model is based. Nevertheless, the EAD phenomenon and variations of the repolarization phase are well captured by the much simpler PLAMIC model.

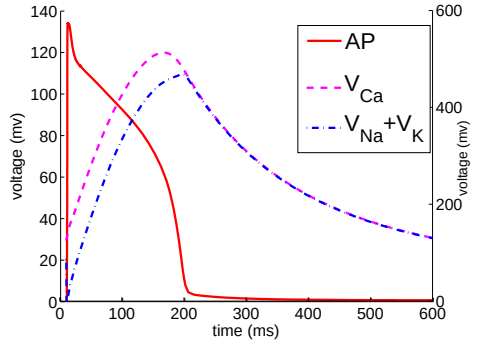

(A) Normal AP from LRd model.

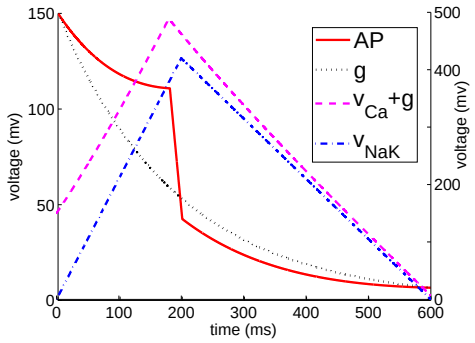

(B) Normal AP from PLAMIC model.

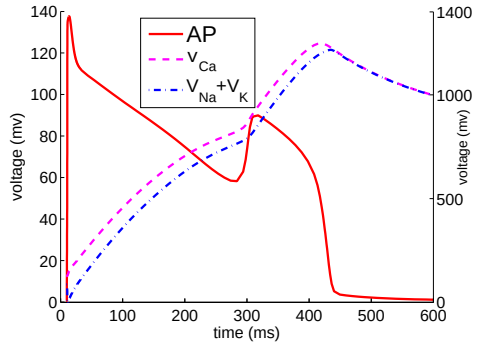

(C) EAD caused by Bay K 8644.

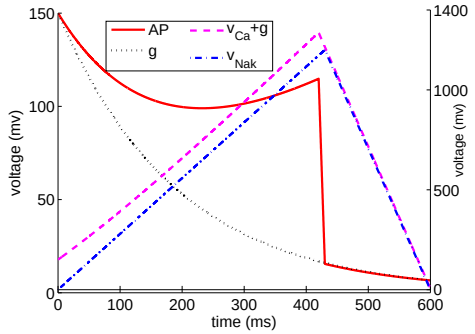

(D) EAD from PLAMIC model.

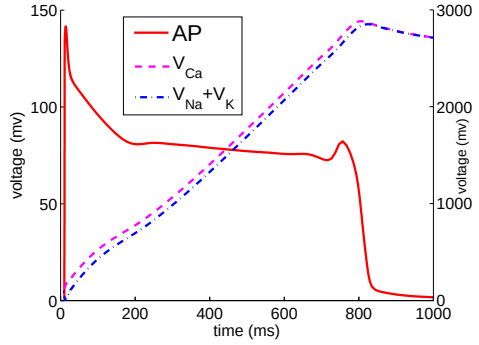

(E) EAD caused by cesium.

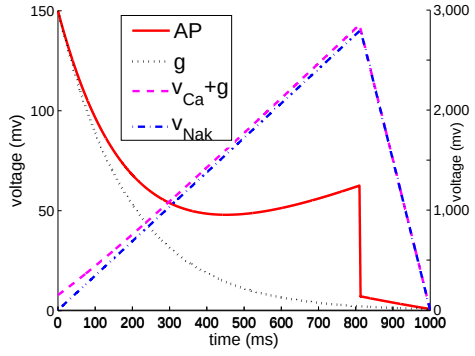

(F) EAD from PLAMIC model.

Fig. 8. Comparison of AP curves from LRd and the PLAMIC model

To validate Theorem 1, formulated for the PLAMIC model, we need only focus on case I since the condition $t^{\mathrm{Ca}}_{\max} < t^{\mathrm{NaK}}_{\max}$ is always true in the LRd model. We also need to reformulate (the last condition of) Theorem 1 for the following reason. In the LRd model, v^{Ca}_{max}, the maximum value of V_{ca} during one AP cycle, serves as the sole contributor to the positive portion of the voltage. In the PLAMIC model, however, the positive part is composed of the linear function $v_{Ca}(t)$ and the decay $g(t)$. Thus, when calculating the slope a^{c}_1 in the LRd model, it is not accurate to use v^{Ca}_{max} directly. Rather, a a "decay" factor given by $V_{max}e^{Ct^{Ca}_{max}}$ should be subtracted from v^{Ca}_{max}.

The reformulation of Theorem 1 is given in Eqn. 15, where $\tilde{a}^{\mathrm{c}}_1$ is the corrected slope and *offset* is a constant used to ensure a non-negative AP value, as in the PLAMIC model.

$$\begin{aligned} &t^{\mathrm{Ca}}_{\max} > \tfrac{1}{D}\ln(\tfrac{a^{\mathrm{k}}_1 - \tilde{a}^{\mathrm{c}}_1}{V_{\max}D}) \\ &\text{where } \tilde{a}^{\mathrm{c}}_1 = \tfrac{v^{\mathrm{Ca}}_{\max} + offset - V_{\max}e^{Dt^{\mathrm{Ca}}_{\max}}}{t^{\mathrm{Ca}}_{\max}} \\ &a^{\mathrm{k}}_1 = \tfrac{v^{\mathrm{NaK}}_{\max}}{t^{\mathrm{NaK}}_{\max}} \end{aligned} \tag{15}$$

In order to test the validity of the derived condition for EAD occurrence given by Eqn. 15, we have assembled a test suite of LRd simulation data consisting of one normal AP and seven APs with variable EADs. The simulation results for both normal AP and abnormal APs are presented in Fig.9. The top panel shows the AP curves and the bottom panel shows $-(V_{\mathrm{Na}} + V_{\mathrm{K}})$ and V_{Ca} as defined by Eqn. 3.

Let $T^{\mathrm{Ca}}_{\max} \equiv \frac{1}{D}\ln(\frac{a^{\mathrm{k}}_1 - \tilde{a}^{\mathrm{c}}_1}{V_{\max}D})$ be the *threshold value* for the LRd model. That is, according to Def. 1 and Thm. 1, an LRd AP should be EAD-producing if and only if $t^{\mathrm{Ca}}_{\max} > T^{\mathrm{Ca}}_{\max}$.[3] Note that since C and $V_{\max}$ are fixed for the LRd model, $T^{\mathrm{Ca}}_{\max}$ is a function of $a^{\mathrm{c}}_1 - \tilde{a}^{\mathrm{k}}_1$, the slope difference.

For each AP, we calculate $a^{\mathrm{c}}_1 - \tilde{a}^{\mathrm{k}}_1$ using the data points $(t^u_{\max}, v^u_{\max})$, $u \in \{Ca, NaK\}$, obtained via numerical simulation from the LRd model, and calculate the threshold time $T^{\mathrm{Ca}}_{\max}$ derived from our formal analysis. This allows us to then compare the $t^{\mathrm{Ca}}_{\max}$ values with the $T^{\mathrm{Ca}}_{\max}$ values. The results of these comparisons are given in Fig. 10, where we plot $t^{\mathrm{Ca}}_{\max}$ and $T^{\mathrm{Ca}}_{\max}$ as a function of the slope difference $a^{\mathrm{c}}_1 - \tilde{a}^{\mathrm{k}}_1$.

As can be seen in Fig. 10, for all APs with EAD, we have that $t^{\mathrm{Ca}}_{\max} > T^{\mathrm{Ca}}_{\max}$. Conversely, for all APs without EAD (only one such AP in our data set), $t^{\mathrm{Ca}}_{\max} < T^{\mathrm{Ca}}_{\max}$. Physiologically, these results suggest that the cells generating EADs spend an amount of time greater than the threshold in letting calcium accumulate and thereby dominate the effects of repolarizing potassium in order to produce such abnormal secondary depolarization. Regardless of the underlying physiology, the results of Fig. 10 demonstrate that Theorem 1 can be used as a valid classifier for EAD prediction, as suggested by the formal analysis.

[3] The other conditions required by Theorem 1 for EAD occurrence, $a^{\mathrm{k}}_1 < a^{\mathrm{c}}_1 < (a^{\mathrm{k}}_1 - V_{\max}D)$, are needed to ensure the existence of a positive real solution for t and are not considered here.

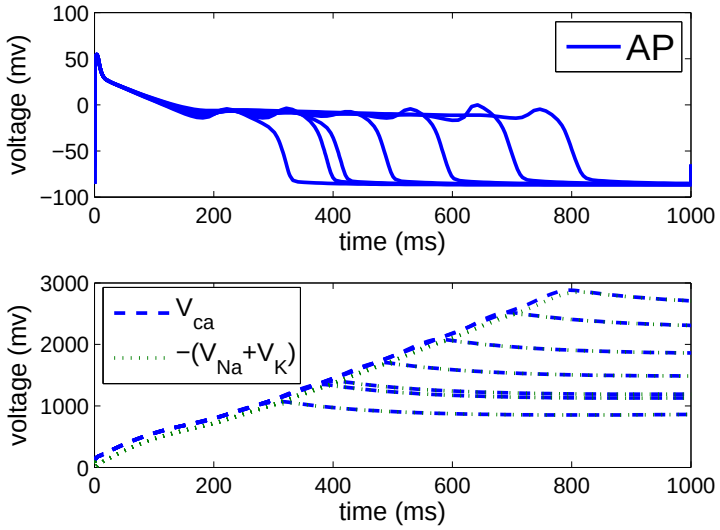

Fig. 9. Simulation of normal AP and APs including EAD with variable timing and severity.

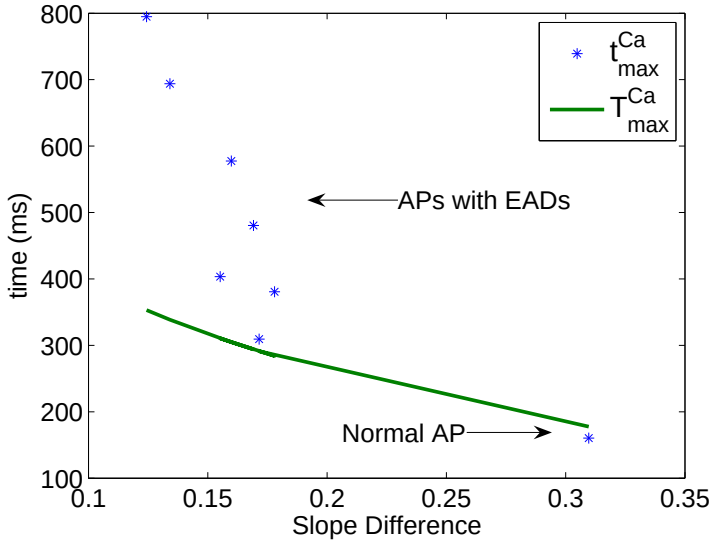

Fig. 10. Validation of the Theorem 1 classification rule for EADs.

5 Discussion and Conclusions

In this paper, we presented the PLAMIC model, a new, simplified model of the action potential in excitable cells. Despite its simplicity and piecewise-linear nature, the PLAMIC model preserves ties to main ionic species and the time course of their contributions to the AP. This allowed us to analyze biological phenomena of clinical importance: early afterdepolarizations (EADs). Unlike the original, highly nonlinear system of equations typically used to model an AP, the PLAMIC model proved amenable to formal analysis.

Specifically, with the PLAMIC model, we were able to explore the parameter space, without having to rely on exhaustive simulations, and to derive basic rules for the conditions under which EADs may occur. Overall, such conditions relate to the subtle balance of different ionic currents during the plateau phase of the repolarization process. While this result is somewhat intuitive and not surprising, to the best of our knowledge, our study is the first to formalize it and to provide quantitative rules for prediction of normal and EAD-containing APs based on the abstracted represenation of the contributing ionic currents. We successfully validated the classification rules obtained by formal analysis with the PLAMIC model by computer simulations with widely accepted, detailed nonlinear AP models.

The utility of the PLAMIC model is rooted in its direct links to experimentally measurable parameters, and the relatively easy derivation of the EAD classification rules for a wide range of AP shapes and different cell types and species. Such a prediction tool can be very useful in designing new anti-arrythmic therapies and in confirming the safety of any genetic or pharmacological manipulations of excitable cells that may lead to alterations in the balance of ionic currents.

There are several limitations of the PLAMIC model. First, due to its simplicity, the AP curves are only qualitatively reproduced. Second, as the PLAMIC model studies the *overall contribution* of an ionic current to changes in the AP; details about the components of a current (steady-state behavior, kinetics parameters), which may be important, are lacking. Such details can perhaps be inferred to some degree from the simple PLAMIC parameters $(t_{\max}, v_{\max})$ based on the different physiological features of detailed currents.

Future work includes validation of the PLAMIC model using actual experimental data with relevant statistical measures. Furthermore, we will explore the derivation of a more accurate excitable-cell model for EAD prediction, yet one that retains the possibility of formal analysis. Our work in using hybrid automata to model excitable cells [10] is one possible formal framework for this research direction.

References

1. F. Charpentier, E. Drouin, C. Gauthier, and H. Le Marec. Early after/depolarizations and triggered activity: mechanisms and autonomic regulation. *Fundam Clin Pharmacol*, 7(1):39–49, 1993.

2. W.T. Clusin. Calcium and cardiac arrhythmias: Dads, eads, and alternans. *Crit Rev Clin Lab Sci*, 40(3):337–75, Jun 2003.
3. P. F. Cranefield and R. S. Aronson. *Cardiac arrhythmias: the role of triggered activity and other mechanisms.* Futura Publishing Company, 1988.
4. H.A. Fozzard. Afterdepolarizations and triggered activity. *Basic Res Cardiol*, 87 Suppl 2:105–13, 1992.
5. M. Hiraoka, A. Sunami, F. Zheng, and T. Sawanobori. Multiple ionic mechanisms of early afterdepolarizations in isolated ventricular myocytes from guinea-pig hearts. *QT Prolongation and Ventricular Arrhythmias.*, pages 33–34, 1992.
6. A. L. Hodgkin and A. F. Huxley. A quantitative description of membrane currents and its application to conduction and excitation in nerve. *J Physiol*, 117:500–544, 1952.
7. N. Homma, M.S. Amran, Y. Nagasawa, and K. Hashimoto. Topics on the na+/ca2+ exchanger: involvement of na+/ca2+ exchange system in cardiac triggered activity. *J. Pharmacol Sci*, 102(1):17–21, 2006.
8. C.T. January and A. Moscucci. Cellular mechanism of early afterdepolarizations. *QT Prolongation and Ventricular Arrhythmias.*, pages 23–32, 1992.
9. C. H. Luo and Y. Rudy. A dymanic model of the cardiac ventricular action potential: I. simulations of ionic currents and concentration changes. *Circ Res*, 74:1071–1096, 1994.
10. P. Ye, E. Entcheva, S.A. Smolka, and R. Grosu. A cycle-linear hybrid-automata model for excitable cells. *IET Systems Biology*, 2(1):24–32, Jan 2008.
11. J. Zeng and Y. Rudy. Early afterdepolarizations in cardiac myocytes:mechanism and rate dependence. *Biophysical J.*, 68:949–964, 1995.